


RESEARCH ARTICLE

Environmental vibrio phage–bacteria interaction networks reflect the genetic structure of host populations

Karine Cahier^{1,2} | Damien Piel^{1,2} | Rubén Barcia-Cruz^{2,3} |
David Goudenège^{1,2} | K. Mathias Wegner⁴ | Marc Monet⁵ |
Jesús L. Romalde^{3,6} | Frédérique Le Roux^{1,2} 

¹Ifremer, Unité Physiologie Fonctionnelle des Organismes Marins, ZI de la Pointe du Diable, Plouzané, France

²Sorbonne Université, CNRS, UMR 8227, Integrative Biology of Marine Models, Station Biologique de Roscoff, Roscoff cedex, France

³Department of Microbiology and Parasitology, CIBUS-Faculty of Biology, Universidade de Santiago de Compostela, Santiago de Compostela, Spain

⁴AWI - Alfred Wegener Institut - Helmholtz-Zentrum für Polar- und Meeresforschung, Coastal Ecology, Waddensea Station Sylt, List, Germany

⁵Institut Pasteur, Université Paris Cité, Plate-forme Technologique Biomics, Paris, France

⁶Cross-Disciplinary Research Center in Environmental Technologies (CRETUS), Universidade de Santiago de Compostela, Santiago de Compostela, Spain

Correspondence

Frédérique Le Roux, Equipe Génomique des Vibrios, UMR 8227, Integrative Biology of Marine Models, Station Biologique de Roscoff, CS 90074, F-29688, Roscoff cedex, France.
Email: fleroux@sb-roscoff.fr

Funding information

Agence Nationale de la Recherche, Grant/Award Numbers: ANR-10-INBS-09, ANR-20-CE35-0014; H2020 European Research Council, Grant/Award Number: 884988; Infrastructures en Biologie Santé et Agronomie; Spanish Ministerio de Ciencia e Innovación, Grant/Award Number: BES-2017-079730

Abstract

Phages depend on their bacterial hosts to replicate. The habitat, density and genetic diversity of host populations are therefore key factors in phage ecology, but our ability to explore their biology depends on the isolation of a diverse and representative collection of phages from different sources. Here, we compared two populations of marine bacterial hosts and their phages collected during a time series sampling program in an oyster farm. The population of *Vibrio crassostreae*, a species associated specifically to oysters, was genetically structured into clades of near clonal strains, leading to the isolation of closely related phages forming large modules in phage–bacterial infection networks. For *Vibrio chagasii*, which blooms in the water column, a lower number of closely related hosts and a higher diversity of isolated phages resulted in small modules in the phage–bacterial infection network. Over time, phage load was correlated with *V. chagasii* abundance, indicating a role of host blooms in driving phage abundance. Genetic experiments further demonstrated that these phage blooms can generate epigenetic and genetic variability that can counteract host defence systems. These results highlight the importance of considering both the environmental dynamics and the genetic structure of the host when interpreting phage–bacteria networks.

INTRODUCTION

Phages, the viral predators of bacteria, constitute the most abundant and diverse biological entities in the ocean and are thought to play a significant role in controlling the composition of microbial communities (Breitbart et al., 2018; Brum & Sullivan, 2015). As

obligate parasites, phages depend on their bacterial hosts to thrive in the environment and therefore the habitat, density and genetic diversity of host populations are expected to be key determinants of phage ecology. Phage ecology encompasses the breadth of host strains a phage is capable of infecting (host range), as well as adsorption, production and dispersion efficiency in the ecosystem (phage–predator load). The ecology of phages in marine environments remains

Karine Cahier and Damien Piel contributed equally to this study.

poorly understood, but such knowledge is important for understanding how they control the expansion of bacterial populations in healthy natural ecosystems and for devising phage applications in disease ridden aquaculture settings (Gordillo Altamirano & Barr, 2019; Kortright et al., 2019; Nobrega et al., 2015).

The farming of Pacific oysters is a prime example of an aquaculture setting susceptible to disease, with the *Vibrionaceae* (hereafter referred to as ‘vibrios’) being the best described bacteria associated with oyster diseases (Le Roux et al., 2015). The ecology, diversity, and population structure of vibrios have been extensively studied (reviewed by Cordero & Polz, 2014, Le Roux et al., 2016). Despite their very broad genomic diversity, vibrios fall into well-defined phylogenetic clusters that are specifically associated with organic particles or host organisms, or correspond to free-living forms in the water column (Hunt et al., 2008; Szabo et al., 2012). These phylogenetic clusters represent distinct populations with respect to gene flow (Hehemann et al., 2016; Shapiro et al., 2012) and interactions with other organisms (social/behavioural networks) (Cordero, Ventouras, et al., 2012; Cordero, Wildschutte, et al., 2012; Hehemann et al., 2016; Yawata et al., 2014) and are predominantly congruent with described *Vibrio* species (Preheim et al., 2011), although with finer evolutionary divergence (Shapiro et al., 2012). Following this finer distinction, here we define ‘populations’ as corresponding to members of a vibrio species isolated from the same location.

By investigating the disease ecology of vibrios in an oyster farming area, we showed that the onset of disease in oysters is associated with progressive replacement of diverse benign colonizers by members of a virulent population, assigned to *V. crassostreae* (Lemire et al., 2015). Although genetically diverse, most members of this population can cause the disease. *V. crassostreae* was abundant in diseased animals and nearly absent in the surrounding seawater, suggesting that its primary habitat is the oyster (Bruto et al., 2017). The distribution of *V. crassostreae* in the tissues and circulatory system of oysters revealed a positive association with the hemolymph (blood), supporting the conclusion that this population is adapted to overcome the immune system of the oysters. This was later confirmed by the identification of virulence factors involved in hemocyte (immune cell) cytotoxicity (Piel et al., 2020; Rubio et al., 2019).

An important consequence of the population framework outlined above is that it allows analysis of environmental dynamics of populations, for example, blooms and busts triggered by specific ecological conditions. We observed that vibrio populations are highly dynamic in the natural ecosystem (Bruto et al., 2017), presumably in part due to predation by phages (Piel et al., 2022). We isolated a large collection of *V. crassostreae* and vibriophage strains from an oyster

farm during a 5-month time-series sampling program. Cross-infection experiments of roughly 82,000 host-phage pairs revealed a low rate of lytic interaction (2.2%), with interconnected groups of phages and hosts (or ‘modules’). These modules involved genomic clusters of phages (taxonomically assigned to the genus rank) that adsorb on distinct phylogenetic clades within the *V. crassostreae* species, suggesting the existence of clade-specific receptor(s) and genus-specific receptor binding protein(s).

It is unclear, however, whether the structure of phage–bacteria infection networks in large modules is a specific characteristic of *V. crassostreae* or a general feature of phage–vibrio interactions. A study exploring diverse populations of vibrios and their phages revealed that singleton modules of interaction (one phage infecting only one strain) were prevalent, highlighting a remarkably narrow host range of phages with respect to their local hosts in the environment (Kauffman et al., 2022). Only a few larger modules were described involving (1) broader host range phages that infect strains from diverse populations, and (2) diverse phages that exclusively infect *V. breoganii*, an algae specialist (Corzett et al., 2018). This suggested that divergence in bacterial ecology, for example, the divergence between host-associated and free-living lifestyles, can be reflected in the topography of the interaction network and host range of the phages (Kauffman et al., 2022).

To further investigate the connection between ecology, genetic diversity and infection networks, here, we compare the structure of phage–bacteria interactions involving *V. crassostreae* and *V. chagasii*. *V. chagasii* was chosen because previous data suggest that its habitat and lifestyle diverge from those of *V. crassostreae*, although the two populations can co-infect the same animal (Bruto et al., 2017). First, the relative abundance of *V. chagasii* in oysters has been reported to resemble that in surrounding seawater. Second, this population preferentially occurred in the free-living (1–0.2 μm) fraction of seawater and oyster digestive glands, where food particles are concentrated in filter feeding oysters (Froelich & Noble, 2014). The presence of *V. chagasii* in the digestive gland is thus likely due to passive transfer by filter feeding and this population might rather bloom in seawater. To directly compare *V. crassostreae* and *V. chagasii*, we analysed the dynamics of *V. chagasii* and their vibriophages in the same time series previously used to describe the *V. crassostreae*–phage infection network (Piel et al., 2022). We combined cultivation, comparative genomics and molecular genetics to analyse a large collection of bacterial isolates and their phages. This allowed determination of crucial parameters of phage ecology by addressing how different host ecologies can feed back on genetic diversity and the structure of the resulting host–phage interaction networks.

EXPERIMENTAL PROCEDURES

Sampling

Sampling was performed at the same time as for Piel et al. (2022). Briefly, samples were collected from an oyster farm located in the Bay of Brest (Pointe du Château, 48°20' 06.19" N, 4° 19' 06.37" W) every Monday, Wednesday and Friday from 3 May to 11 September 2017. Specific pathogen free (SPF) juvenile oysters (Petton et al., 2015) were deployed in the field in batches of 100 animals. When the first mortalities were observed in the first batch, another batch of SPF animals was placed in the field, leading to the consecutive deployment of seven batches from 26 April to 11 September. Oyster mortalities were recorded on each sampling day. Seawater temperature reached 16°C on 22 May, a previously observed threshold for oyster mortalities (de Lorgeril et al., 2018). Mortalities began on 29 May and persisted until 25 August. On each sampling date, five living oysters were collected from a batch showing less than 50% mortality. The animals were cleaned, shucked, weighed and 2216 Marine Broth (MB) was added (10 mg/mL) for homogenization using an ultra-turrax. The 100 µL of the homogenate was used for vibrio isolation, with the remaining volume centrifuged (10 min, 17,000 g) and the supernatant filtered through a 0.2 µm filter and stored at 4°C until the phage isolation stage. Two litres of seawater were collected and size fractionated as previously described (Bruto et al., 2017). Bacterial cells from 0.2 µm filters were suspended in 2 mL MB and 100 µL of this suspension was used for vibrio isolation. The iron chloride flocculation method was used to generate 1000-fold concentrated viral samples from 2 L passed through a 0.2 µm filter, following the previously described protocol (Kauffman et al., 2018). Virus-flocculates were suspended in 2 mL 0.1 M EDTA, 0.2 M MgCl₂, 0.2 M oxalate buffer at pH 6 and stored at 4°C until the phage isolation stage.

Vibrio isolation, identification and genome analysis

Isolation and identification

Vibrios from seawater or oyster tissues were selected on thiosulfate-citrate-bile salts-sucrose agar (TCBS). Roughly, 48 colonies were randomly picked from each plate and re-isolated once on TCBS, then on 2216 Marine agar (MA). Colonies were screened by PCR targeting the *r5.2* gene encoding for a regulator (Lemire et al., 2014). PCR positive isolates were grown in MB and stored at -80°C in 10% DMSO. Bacteria were grown overnight in 5 mL MB and DNA extracted using an extraction kit (Wizard, Promega) according to the manufacturer's instructions. Taxonomic assignment

was further refined by *gyrB* gene sequencing to identify *V. crassostreae* and *V. chagasii* isolates. The partial *gyrB* gene was amplified using degenerate primers (Table S5), Sanger sequenced (Macrogen), with sequences manually corrected by visualization of chromatograms. Sequences were aligned with Muscle and phylogenetic reconstruction was performed with RAxML version 8 GTR model of evolution, a gamma model and default parameters (Stamatakis, 2006).

Genome sequencing, assembly and annotation

V. chagasii libraries were prepared from 500 ng of genomic DNA using MGIEasy Universal DNA Library Prep Set following the manufacturer's instruction. The 100 bp paired-end library pools were circularized and sequenced using DNBSEQ-G400 (BGI) by the Biomics platform at the Pasteur Institute (Paris, France). Reads were trimmed using Trimmomatic v0.39 (LEADING:3, TRAILING:3, SLIDINGWINDOW:4:15, MINLEN:36) (Bolger et al., 2014). *De novo* read assembly was performed using Spades version 3.15.2 (--careful --cov-cutoff auto -k 21,33,55,77 -m 10). In order to confirm BGI sequencing quality, we compared these assembly results with those obtained for 20 of the same *V. chagasii* strains sequenced by Illumina HiSeq using QUASt v5.0.2 (Gurevich et al., 2013) (Table S6). We confirmed the previous benchmark studies showing similar sequencing and assembly qualities across both platforms (Foux et al., 2021). Computational prediction of coding sequences and functional assignments were performed using the automated annotation pipeline implemented in the MicroScope platform (Vallenet et al., 2020). Phage defence gene annotation was performed using Defense-Finder version 1.0.8 (Tesson et al., 2022) with MacSyFinder models version 1.1.0 and default options. Persistent genome phylogeny was undertaken using the PanACoTA workflow (Perrin & Rocha, 2021) version 1.3.1-dev2 with mash (version 2.3) distance filtering from 0 to 0.3, prodigal version 2.6.3 for syntactic annotation, mmseqs version 2.11. e1a1c for gene clustering, mafft version 7.407 for persistent genome alignment defined as 90.0% of all genomes in each family and IQ-TREE (Nguyen et al., 2015) version 2.0.3 based on GTR model and 1000 bootstrap for tree construction.

Comparative genomics

The average nucleotide identity (ANI) value of genomes was determined using fastANI version 1.32 (fragment length 500) (Jain et al., 2018). *V. crassostreae* and *V. chagasii* core, variable, accessory and specific genomes were established using

mmseqs2 reciprocal best hit version 13-45111 with 80% identities on 80% coverage thresholds (Steinegger & Soding, 2018). Synteny plots were generated using dedicated python scripts based on the 'DNA Features Viewer' library (<https://github.com/Edinburgh-Genome-Foundry/DnaFeaturesViewer>) and clinker for conservation representation (<https://github.com/gamcil/clinker>).

Phage isolation, identification and genome analysis

Phage isolation

We used the 194 and 252 isolates of *V. crassostreae* and *V. chagasii* respectively as 'bait' to isolate phages from the same date of sampling from 20 mL seawater equivalents of viral concentrate (1000 \times) or oyster tissues (0.1 mg). Phage infection was assessed by plaque formation in soft agar overlays of host lawns mixed with both viral sources. For *V. crassostreae*, due to the limited number of co-occurring phages, the collection was completed by isolating viruses from seawater concentrates sampled on several dates (Piel et al., 2022). For *V. chagasii*, we purified one phage from each plaque positive host, representing a final set of 95 phage isolates. To generate high titre stocks, plaque plugs were first eluted in 500 μ L of MB for 24 h at 4°C, 0.2- μ m filtered to remove bacteria, and re-isolated three times on the sensitive host for purification before storage at 4°C and, after the addition of 25% glycerol, at -80°C. High titre stocks (>10⁹ PFU/mL) were generated by confluent lysis in agar overlays and phage concentration was determined by dropping spots of 10-fold serial dilutions onto bacterial host lawns.

Electron microscopy

Following concentration on centrifugal filtration devices (Millipore, amicon Ultra centrifugal filter, Ultracel 30K, UFC903024), 20 μ L of the phage concentrate were adsorbed for 10 min to a formvar film on a carbon-coated 300 mesh copper grid (FF-300 Cu formvar square mesh Cu, delta microscopy). The adsorbed samples were negatively contrasted with 2% uranyl acetate (EMS, Hatfield, PA, USA). Imaging was performed using a Jeol JEM-1400 Transmission Electron Microscope equipped with an Orious Gatan camera at the MERIMAGE platform (Station Biologique, Roscoff, France).

DNA extraction

Phage suspensions (10 mL, >10¹⁰ PFU/mL) were concentrated to approximately 500 μ L on centrifugal filtration devices (30 kDa Millipore Ultra Centrifugal Filter, Ultracel

UFC903024) and washed with 1/100 MB to decrease salt concentration. The concentrated phages were next treated for 30 min at 37°C with 10 μ L of DNase (Promega) and 2.5 μ L of RNase (Macherey-Nagel) at 1000 units and 3.5 mg/mL, respectively. Nucleases were inactivated by adding EDTA (20 mM, pH 8). DNA extractions involved a first protein lysis step (0.02 M EDTA pH 8.0, 0.5 mg/mL proteinase K, 0.5% SDS) for 30 min incubation at 55°C, followed by phenol chloroform extraction and ethanol precipitation. DNA was visualized by agarose gel electrophoresis (0.7% agarose, 50 V, overnight at 4°C) and quantified using QuBit.

Genome sequencing, assembly and annotation

Phages were sequenced by the Biomics platform at the Pasteur Institute (Paris, France). The sequencing library (2 \times 75 bp paired end) was prepared using a TruSeq Illumina kit and sequenced on a NextSeq550 Illumina sequencer. After read trimming conducted with Trimmomatic v0.39 (LEADING:3, TRAILING:3, SLIDINGWINDOW:4:15, MINLEN:36) (Bolger et al., 2014), *de novo* assembly was performed using SPAdes v3.15.2 (-careful -cov-cutoff auto -k 21,33,55,77 -m 10). Vector contamination contigs were excluded using the UniVec Database and the one-contig phage genome was manually decircularized. Syntactic annotation was performed with PHANOTATE v1.5.0 (McNair et al., 2019). Large terminase subunit was identified using DIAMOND v2.0.8.146 (blastp, default parameters) (Buchfink et al., 2021) on previously annotated vibrio large terminase and using HMMSCAN (HMMER v3.3.2, default parameters with evalue $\leq 10^{-3}$) with PFAM profiles (PF03354.17, PF04466.15, PF05876.14, PF06056.14) (Mistry et al., 2021). The phage genome was manually ordered starting from the gene for the large terminase subunit.

The tRNA were identified with tRNAscan-SE v2.0.9 (Chan & Lowe, 2019). Functional annotation used multiple approaches. First, we used HMMSCAN (evalue $\leq 10^{-3}$) with PVOGS profiles (Grazziotin et al., 2017). We also used DIAMOND blastP against first the Nahant collection genomes and then against other bacterial RefSeq (version 212) and phage GenBank genomes (24 June 2022, with 30% identities and 50% coverage) (Buchfink et al., 2021; Kauffman et al., 2018). Finally, we added InterProScan v5.52-86.0 (evalue $\leq 10^{-3}$) and eggNOG v5.0.2 annotation results (Huerta-Cepas et al., 2019; Jones et al., 2014).

Clustering, lifestyle and comparative genomics

We clustered phages using VIRIDIC v1.0r3.6 (default parameters) (Moraru et al., 2020). Intergenicomic

similarities were identified using BLASTn pairwise comparisons. Virus assignment into family ($\geq 50\%$ similarities), genera ($\geq 70\%$ similarities) and species ($\geq 95\%$ similarities) ranks followed the International Committee on Taxonomy of Viruses (ICTV) genome identity thresholds. Phage lifestyle was predicted using BACPHILIP version 0.9.3-alpha and lysogeny associated genes were searched using InterProScan (v.5.52-86.0) based on integrase (IPR002104), resolvase (IPR006119), replicative transposases (IPR004189), and transcriptional repressor domains (IPR010982, IPR010744, IPR001387, IPR032499). The absence of prophage integration was also checked using BLASTn searches between both phage and bacterial genomes (evalue ≤ 0.01) (Hussain et al., 2021). All comparative genomic analyses were conducted using MMseqs2 version 13-45111 for protein clustering (Steinegger & Soding, 2018), FAMSA version 1.6.2 for gene/protein alignments (Deorowicz et al., 2016) and IQ-TREE version 2.1.2 for phylogenetic tree construction (Nguyen et al., 2015).

Host range determination

Single-phage-by-single-host host range infection assay

Host range assays were carried out using an electronic multichannel pipette by spotting 5 μL of the phage suspension normalized at 2×10^5 PFU/mL (10^3 PFU/spot) on the agar overlay inoculated with the tested host. Plates were incubated overnight at RT and plaque formation was observed after 24 h. Spot assays were performed for *V. chagasii*, first by infecting 358 vibrio strains (252 *V. chagasii* + 106 strains belonging to other vibrio populations) with 95 phages in duplicate. Then, the host range of 49 selected phages was confirmed on 136 *V. chagasii* hosts. Concerning *V. crassostreae*, results were obtained in (Piel et al., 2022).

Efficiency of plating

Ten-fold serial dilutions of phages from a high titre stock ($>10^9$ PFU/mL) were prepared and 10 μL of each dilution were pipetted onto bacterial host lawns. The efficiency of plating (EOP) was calculated as the ratio between the titre of a phage on a given strain compared to the titre of the same phage on its reference strain (host used to isolate and produce the phage).

Adsorption estimation

Phage adsorption experiments were performed as previously described (Hyman & Abedon, 2009). Phages were mixed with exponentially growing cells (OD 0.3;

10^7 CFU/mL) at a MOI of 0.01 and incubated at RT without agitation. At different time points, 250 μL of the culture was transferred into a 1.5 mL tube containing 50 μL of chloroform and centrifuged at 17,000 g for 5 min. The supernatant was 10-fold serially diluted and drop spotted onto a fresh lawn of a sensitive host to quantify the remaining free phage particles. In this assay, a drop in the number of infectious particles at 15 or 30 min indicates bacteriophage adsorption.

Statistical analyses

Statistical analyses were based on linear models (LM) when data were normally distributed or on negative binomial generalized linear models (negbin GLM) when data were left skewed. Correlations were based on non-parametric Spearman's rank correlations. Paired tests were analysed as linear mixed models adding the paired factor as a random intercept. All analyses were performed using the R statistical environment (v.4.0.5).

Molecular microbiology

Strains and plasmids

All plasmids and strains used or constructed in the present study are described in Tables S7 and S8. *V. chagasii* isolates were grown in Marine broth (MB) or LB + 0.5 M NaCl at RT. *Escherichia coli* strains were grown in LB at 37°C. Chloramphenicol (Cm; 5 or 25 $\mu\text{g}/\text{mL}$ for *V. chagasii* and *E. coli*, respectively), thymidine (0.3 mM) and diaminopimelate (0.3 mM) were added as supplements when necessary. The P_{BAD} promoter was induced by the addition of 0.2% L-arabinose to the growth media and repressed by the addition of 1% D-glucose. Conjugation between *E. coli* and *V. chagasii* was performed at 30°C as described previously (Le Roux et al., 2007).

Cloning

For vibrio knock outs, all cloning in the suicide vector pSW7848T was performed using Herculase II fusion DNA polymerase (Agilent) for PCR amplification and the Gibson Assembly Master Mix (New England Biolabs, NEB) according to the manufacturer's instructions. For recombination of the 409E50-1 phage, a 227 bp region flanking the SNP (T in 409E50-1, G in other phages from species 26) was amplified using the Herculase II and DNA from the 521E56-1 phage and cloned by Gibson Assembly in pMRB (Le Roux et al., 2011) instead of the *gfp* gene. All cloning was first confirmed by digesting plasmid minipreps with

specific restriction enzymes and second by sequencing the insert (Eurofins).

Vibrio mutagenesis

Knock out was performed by cloning 500 bp fragments flanking the pSW7848T region (Le Roux et al., 2007). This suicide vector encodes the *ccdB* toxin gene under the control of an arabinose-inducible and glucose-repressible promoter, P_{BAD} . Selection of the plasmid-borne drug marker on Cm and glucose resulted from integration of pSW7848T in the genome. The second recombination leading to pSW7848T elimination was selected on arabinose-containing media.

Phage mutagenesis

Recombinant phage (T > G in p0076 of phage 409E50-1) was engineered using double crossing over with a plasmid carrying a 227 region of homology to the phage genome 521E56-1 (Figure 5D). This plasmid, or as control the original pMRB-*gfp*, was transferred by conjugation to strain 50_O_409. Plate lysates were generated by mixing 100 μ L of an overnight culture of the transconjugant with the 409E50-1 phage and plating in 5 mL agar overlay. After the development of a confluent lysis of lawns, the lysate was harvested by addition of 7 mL of MB and shredding of the agar overlay and stored ON at 4°C for diffusion of phage particles. The lysates were next centrifuged, the supernatant filtered through 0.2 μ m filter and stored at 4°C. We could not enrich the recombinant phages by infecting LS strains because these strains confer epigenetic protection to the 409E50-1 phage. We therefore performed several successive passages of the phage on the strain carrying the plasmid, testing the infectivity of the phages on the original strain and the LS strain at each passage. After three passages, a different titre between the putative recombinant and controls was observed. The p0076 gene was PCR amplified using single plaque as template (eight recombinant or eight control phages) and primers flanking the 227 region in the phage genome (external primers). The SNP was confirmed by sequencing. Three control or recombinant phages were tested by EOP on four LS strains in addition to the source 50_O_409.

RESULTS AND DISCUSSION

Phage load correlates with *V. chagasii* frequency

We sampled vibrios from juvenile oysters deployed in an oyster farm (Bay of Brest, France) and from the

surrounding seawater on 57 dates over 5 months, including a period with mortality events (Piel et al., 2022). On each sampling date, total vibrios from oysters and seawater were isolated on selective media. Of the 5268 randomly picked colonies, 252 isolates were assigned to *V. chagasii* by sequencing and analysis of the gene encoding the DNA gyrase subunit B. A total of 144 *V. chagasii* isolates were obtained from the 1–0.2 μ m (free-living) seawater fraction, while the remaining 108 isolates were obtained from oyster tissues (Table 1). *V. chagasii* was detected later than *V. crassostreae* and persisted after the disease outbreak, suggesting that a role in oyster disease is unlikely (Figure 1A).

Each of the 252 *V. chagasii* isolates was used as ‘bait’ to detect co-occurring lytic phages from both (1) seawater viral concentrate and (2) oyster tissues (504 combinations tested). Phage infection was assessed by plaque formation in soft agar overlays of host lawns mixed with the viral source (see Section Experimental Procedures). Of the 252 strains, 113 (44.8%) were plaque positive, 59 of which were isolated from seawater and 54 from oysters (Table 1). The vast majority of plaque-forming units (PFUs) were obtained using seawater concentrate as the viral source (2023 PFUs from seawater vs. 35 PFUs from oysters), which could be expected considering that viruses from seawater were concentrated 1000X. The number of phages infecting *V. chagasii* in seawater was estimated to range from 50 L⁻¹ (1 PFU observed on the plate using 20 mL seawater equivalents of viral concentrate 1000X) to more than 5.10³ L⁻¹ depending on the strain and date. Phage load was significantly correlated with *V. chagasii* frequency in both isolation fractions (Figure 1B), consistent with a role of host blooms in driving phage abundance (Kauffman et al., 2022). Twice as many PFUs were obtained using vibrios isolated from oysters as prey (1347 vs. 676 when using vibrio from seawater, Table 1), but this difference was driven by the high proportion of *V. chagasii* isolated from oysters on 25 August (30/108; 30%), with 29 out of every 30 isolates being plaque positive leading to a total of 1088 PFUs. By comparison, the ratio of plaque positive to total number of hosts (18/194, 9.2%) and the number of plaques per host were significantly lower for *V. crassostreae* in both isolation fractions (Table 1). Detection of only 47 PFUs from seawater viral concentrates versus 2023 PFUs for *V. chagasii* confirmed the scarcity of *V. crassostreae* in the seawater. It is noteworthy that during oyster disease at least 50% of oysters die rapidly and massive numbers of *V. crassostreae* will be released into the water column. The low number of PFUs in seawater suggests that vibrios from this population rapidly colonize new animals rather than remaining in the water column.

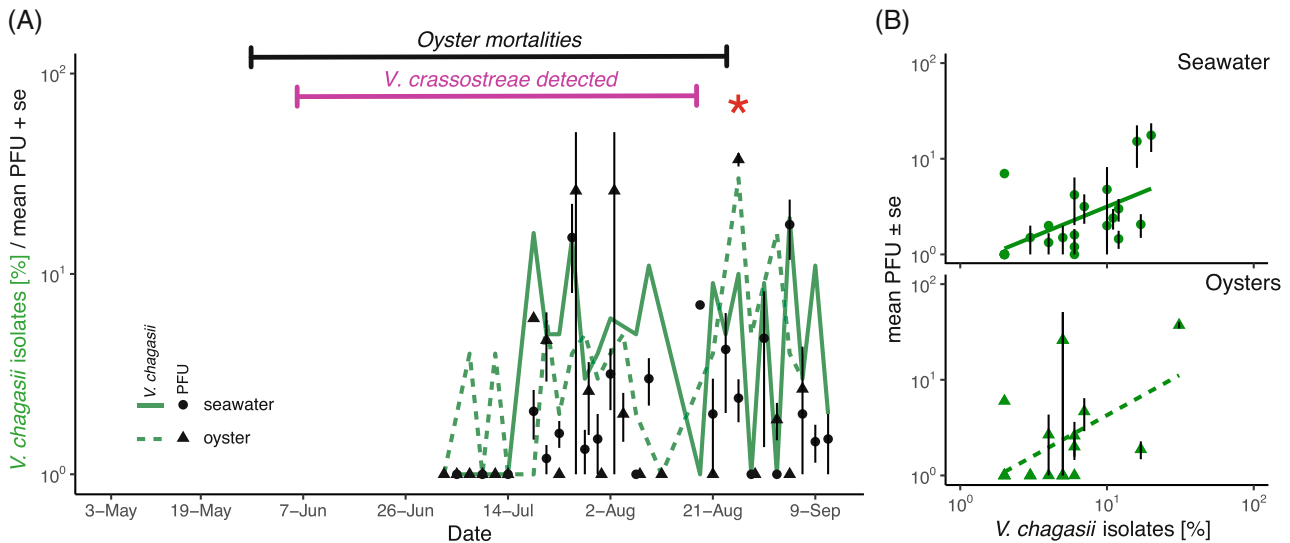


FIGURE 1 Time-series sampling of *V. chagasii* and vibriophages. (A) On each sampling date, vibrios from seawater (1–0.2 μm size fraction) or tissue from five oysters were selected on TCBS and genotyped to identify *V. chagasii* isolates. Oyster mortalities occurred between 29 May and 25 August (black bar) and *V. crassostreae* was detected in oysters from 16 June 16 to 18 August (pink bar). Green lines show the frequency of *V. chagasii* (number of positive isolates out of 48 randomly picked colonies \times 100) in seawater (solid) or oyster tissue (dashed). Each of the *V. chagasii* isolates was used as ‘bait’ to detect co-occurring lytic phages by plaque formation in soft agar overlays of host lawns mixed with viral concentrate from (1) seawater and (2) oyster tissues. Black circles and triangles indicate the mean number \pm se of plaque forming units (PFU) obtained for each plaque positive host using viruses collected from seawater (circles) or oyster tissue (triangles) collected on the same day. The red star indicates the date of the *V. chagasii* bloom (25 August). (B) Correlation between mean number of PFUs and *V. chagasii* frequency for viral concentrates from seawater (upper panel) or oysters (lower panel). Regression lines show similar correlation estimates for both isolation fractions (seawater: estimate = 0.627 ± 0.193 , $t = 3.252$, $p = 0.004$; oyster: estimate = 0.849 ± 0.342 , $t = 2.487$, $p = 0.022$).

(Figure 3A), which led us to group the 49 phages infecting *V. chagasii* into 25 VIRIDIC genera (ANI > 70%) and 41 species (ANI > 95%). By comparison, the higher number of 57 phages isolated using *V. crassostreae* were assigned to only 19 genera and 23 species (Figure 3B), indicative of a higher taxonomic diversity in our collection of *V. chagasii* phages.

Only one genus (Genus 1, Podoviruses, Table S3) contained phages predicted as temperate phages by BACPHILIP (score 0.975). A gene encoding a putative integrase (tyrosine recombinase) was detected in the genomes of all 11 phages in this genus. However, this prediction was contradicted by the absence of integration of the phages in *V. chagasii* genomes. Tyrosine recombinase constitutes a large protein family involved in a wide variety of biological processes (post-replicative segregation, genetic switches and movement of mobile genetic elements including phages) (Smyshlyaev et al., 2021) and functional annotation of these proteins is still limited by their diversity and lack of experimental data. Therefore, the classification of these phages as lysogens will have to be validated experimentally.

We identified a single genus (Genus 10, Table S3) that contains phages infecting both *Vibrio* species (Figure 3A). This genus splits into two VIRIDIC species (identities >95%), the first (species 38) containing a single phage isolated from *V. chagasii* and the second (species 15) containing seven phages isolated

from *V. crassostreae*. Among genes specific to VIRIDIC species 15, we found a gene encoding a protein with a N-terminal phosphoadenosine phosphosulphate reductase (PAPS) domain and a C-terminal DNA N-6-adenine-methyltransferase (Dam) domain (Figure S3). We previously demonstrated that this gene (called PAPS-Dam) is involved in phage counter-defence against the DNA phosphorothioation-based defence system Dnd (Piel et al., 2022). We used Defense-Finder (Tesson et al., 2022) to identify known defence systems in the hosts used to isolate the phages from Genus 10 and found the Dnd_ABC-DEFGH system (Wang et al., 2011) in all *V. crassostreae* but not in *V. chagasii* hosts. This suggested that the PAPS-Dam phage anti-defence system is involved in the adaptation of phages from species 15 to their *V. crassostreae* host.

Some genera of phages isolated from *V. crassostreae* or *V. chagasii* could be clustered in VIRIDIC families (identities >50%). A core proteome phylogeny of the best represented family indicated that phages differentiated from a common ancestor into genus and species in their respective vibrio host species (Figure 3A, Figure S4). Neither *V. crassostreae*-infecting phages nor *V. chagasii*-infecting phages form monophyletic clades, which indicates that phages have jumped several times from one host species to another. To investigate evidence for past recombination among phages, we compared the phylogenetic relationships of

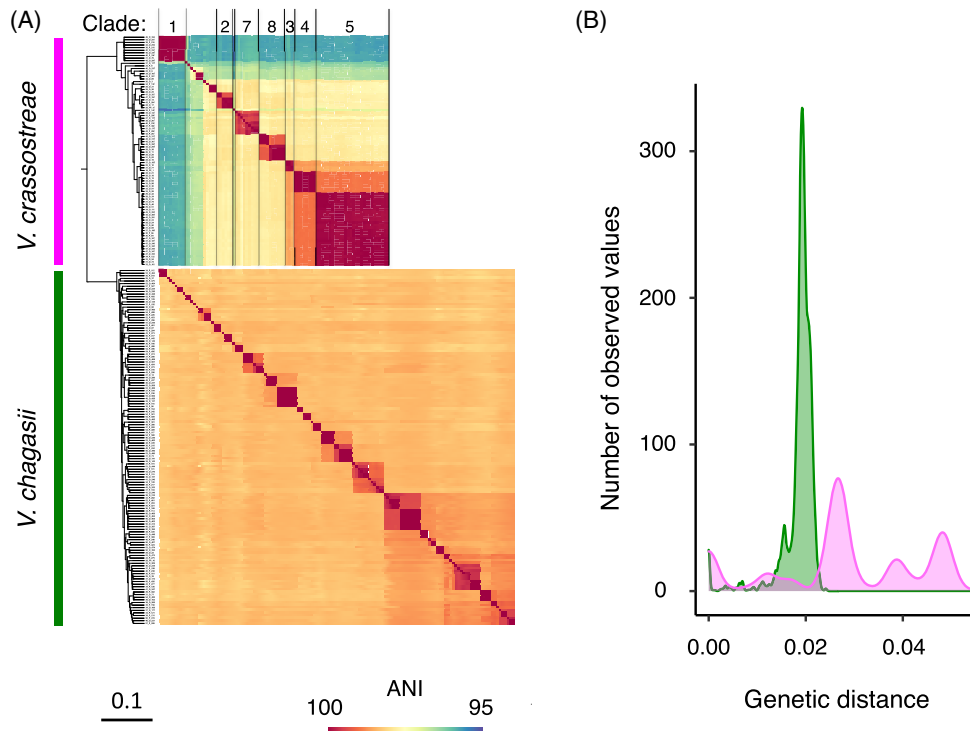


FIGURE 2 Genome diversity of *V. crassostreae* and *V. chagasii*. (A) Core genome phylogeny based on 2689 gene families of 88 *V. crassostreae* and 136 *V. chagasii* isolates from the time series, with pairwise ANI values revealing highly structured clades in *V. crassostreae* but not in *V. chagasii*. Clade numbers refer to the study by Piel et al. (2022). (B) The resulting distribution of pairwise genetic distance within *V. chagasii* (green) and *V. crassostreae* (pink) indicates striking differences between these species (two-sample Kolmogorov–Smirnov test, $D = 0.762$, $p < 0.001$): *V. chagasii* exhibits a unimodal distribution with few clonal strains and a homogenous pairwise genetic distances with a maximum differentiation of 0.024, whereas *V. crassostreae* exhibits a multimodal distribution corresponding to the distinct clades with low within-clade and large between clade genetic distances.

each core protein (Figure S5). Only 3 out of 38 proteins, a large terminase, a DNA binding protein and a putative primase, cluster all *V. crassostreae*-infecting phages in a clade with 56%, 100% and 85% bootstrap values, respectively. Incongruences in other protein tree topologies suggest that recombination has shuffled genes between phages. We speculate that vibrio diversity and coinfection of oysters could enhance genomic diversification of the viral population, promoting phage host jumps, as previously described for gut microbiota (De Sordi et al., 2017).

We analysed host–phage interactions taking the vibrio core genome phylogeny and phage clustering into consideration (Figure 4A). In *V. chagasii*, the size of modules was significantly smaller than in *V. crassostreae* (negative binomial GLM, estimate = 1.234 ± 0.241 , $z = 5.121$, $p < 0.001$). Phages isolated using *V. chagasii* were more diverse than those from *V. crassostreae*, which might at least partially explain the difference in module size. Smaller modules might also indicate higher specialization of phages, that is, a lower number of susceptible hosts. Comparing pairwise number of shared phages and phylogenetic distance, we found that the likelihood of sharing phages was highest at the smallest genetic distances (Figure 4B). Both species

exhibited a multimodal distribution of sharing probabilities reflecting the modular structure of the infection network. However, the distribution of these modes differed substantially between the two species. While *V. chagasii* strains showed a comparatively high sharing probability ($\sim 20\%$) at moderate genetic distances of 0.02, the largest genetic distance with compatible phages was observed for *V. crassostreae* strains at genetic distances larger than 0.04. This suggests a higher degree of specialization of *V. chagasii* phages. In fact, only one phage (382E49-1) out of 49 was able to infect strains with larger genetic distances (>0.024). We therefore conclude that smaller modules in *V. chagasii* are a consequence of the lower number of genetically similar hosts, as well as a higher diversity of the phages coupled to a higher degree of specialization.

With such a narrow host range, phages have to find strategies that increase encounter rates with their host. On the one hand, *V. chagasii* inhabits an open system (seawater), which might require a high viral load to promote phage–bacteria encounters. Individual strains of the most abundant *Vibrio* species have previously been estimated to occur at concentrations of on average 10^3 L^{-1} (Kauffman et al., 2022) and in the present

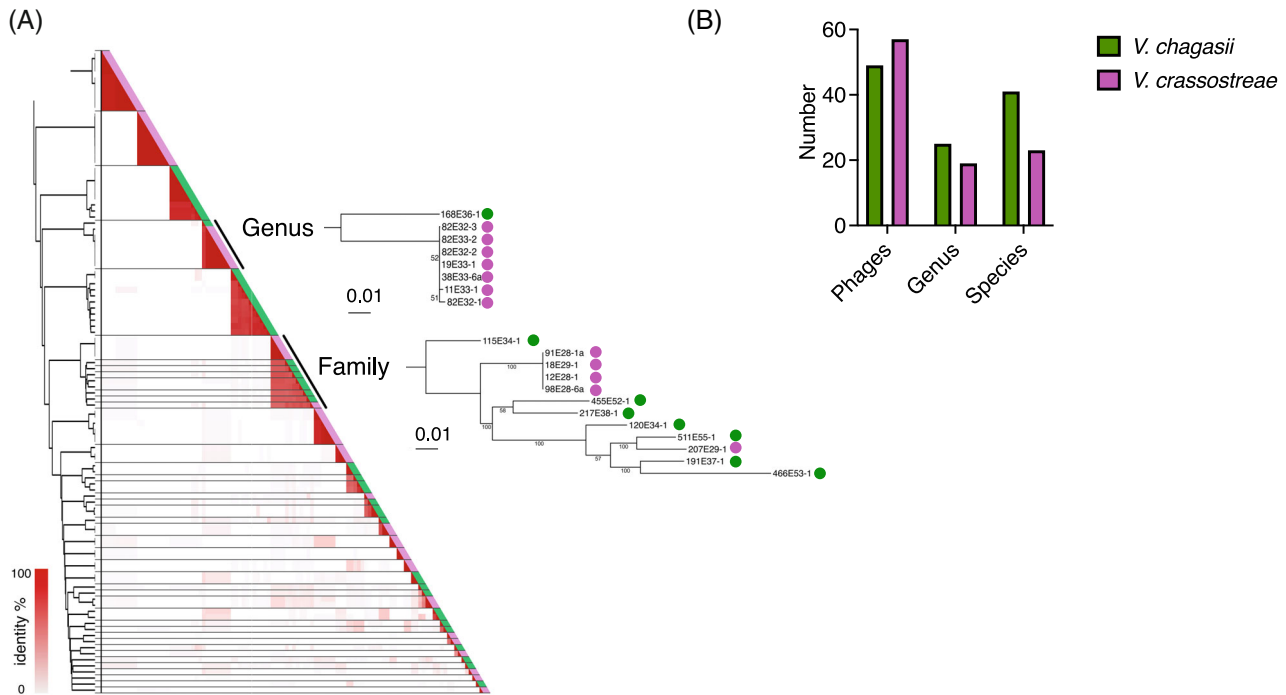


FIGURE 3 Diversity of phages isolated using *V. chagasii* and *V. crassostreae* as hosts. (A) VIRIDIC intergenomic similarity between phage genomes. The 106 phages included in the study were grouped into 43 clusters assigned to VIRIDIC genus rank (>70% identities, indicated with a plain line). Only one genus contains phages isolated using *V. crassostreae* or *V. chagasii*. The phylogenetic tree based on 41 core proteins (25% identities and 80% coverage) shows that this genus splits into two clades, one represented by a single phage isolated from *V. chagasii* and the second containing seven phages all isolated from *V. crassostreae*. Some genera were grouped into clusters assigned to VIRIDIC family rank (>50%). For the larger family, the phylogenetic tree based on 38 core proteins (25% identities and 80% coverage) delineates the phages isolated from *V. crassostreae* and *V. chagasii* populations. (B) The 49 and 57 phages infecting *V. chagasii* and *V. crassostreae* were assigned to 25 and 18 genera and 41 and 23 species, respectively.

study we showed that the number of phages infecting a *V. chagasii* strain could reach 5.10^3 L^{-1} in seawater. On the other hand, the oyster specialist *V. crassostreae* reaches a higher density in the animal host, which might favour physical contact and promote phage infection. Furthermore, as the *V. crassostreae* population is genetically structured by distinct clades of nearly clonal strains, the same phage can potentially infect more hosts. Exploring to what extent clades bloom in distinct oysters, co-occur in the same animal, or bloom sequentially, might be necessary to decipher whether the loss of a specific *V. crassostreae* clade is frequently accompanied by the rise of a population of phages, which would be a clear indication that the latter moderate the population of the former.

Large numbers of phages during blooms generate epigenetic and genetic variability

Blooms of specific strains can dramatically increase the abundances of specific phages as observed in the time series on 25 August (Figures 1A and S1). The only large module observed in the *V. chagasii* phage–bacteria network connecting hosts and phages was

isolated from samples taken on this date (Figure 4A). On the host side, the phylogenetic relationship based on the core genome revealed the grouping of eight strains in a clade with very little intra-clade diversity (2–20 single nucleotide polymorphisms [SNPs] (Figure S6). Seven of these strains were isolated from oysters sampled on 25 August, and the absence of strain-specific genes further confirmed their clonality. The most closely related clade contains a group of four strains with higher diversity (5–823 SNPs, 40 genes specific to strain 52_P_461 and 10 genes specific to strain 37_P_203) that were isolated from seawater collected before and after 25 August. Similarly, among the nine phages with sequenced genomes isolated from samples taken on 25 August, five belong to the same species (species 26, genus 18 Table S3) and differed by a unique SNP (Figure S7). We compared the virulence of these phages for all hosts from the two previously described sister clades using efficiency of plating (EOP), that is, the titre of the phage on a given bacteria compared to the titre on the strain used to isolate the phage (original host) (Figure 5A). This revealed that only phage 409E50-1 showed noticeable variation separating the four strains from the more diverse clade with low susceptibility (LS). These four LS strains showed

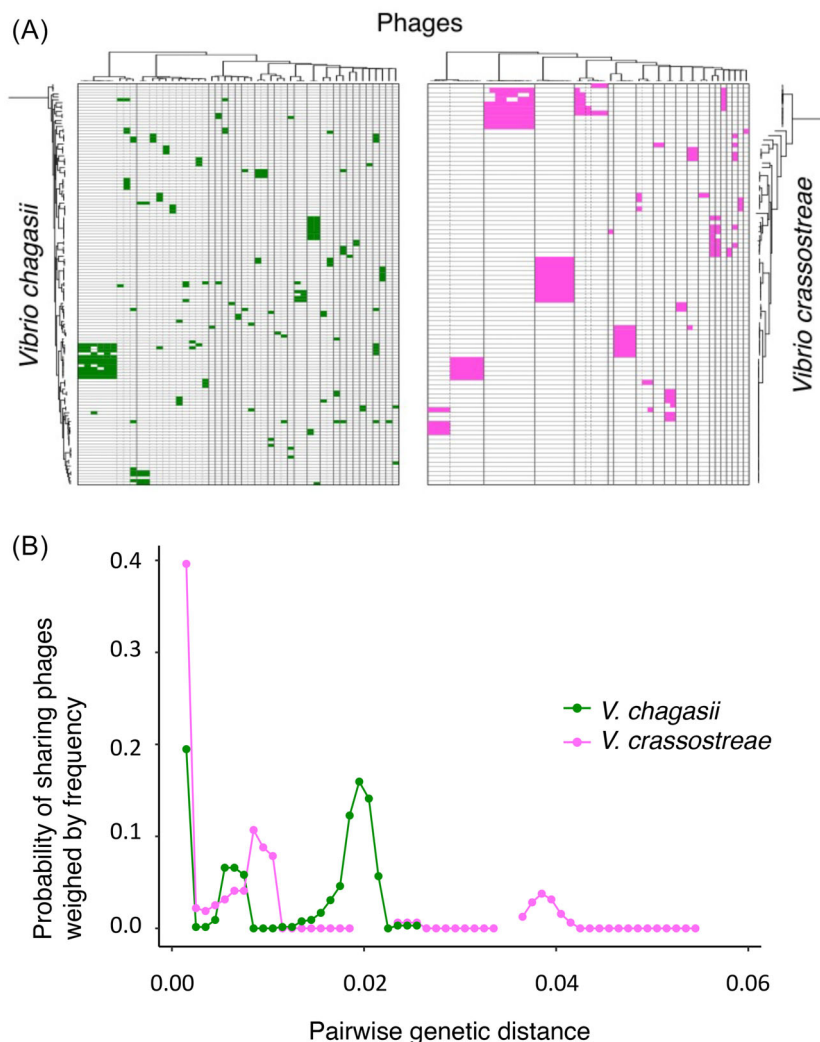


FIGURE 4 Modularity is driven by phylogenetic distances within the host population. (A) Comparisons of the phage–bacteria infection matrix for *V. crassostreae* and *V. chagasii* as hosts. Rows represent sequenced *Vibrio* strains ordered according to the Maximum Likelihood core genome phylogeny of *V. chagasii* ($n = 136$ green matrix) and *V. crassostreae* strains ($n = 88$; pink matrix). Columns represent sequenced phages (49 and 57 isolated from *V. chagasii* and *V. crassostreae*) ordered by VIRIDIC genus (see dendrogram in Figure 3A). Coloured squares indicate killing of the respective vibrio isolate by the phage. Vertical lines represent VIRIDIC genus (solid) and species (dashed). (B) Sharing probability (i.e. proportion of phages shared in all pairs within a window of genetic distances) weighed by the frequency of pairwise comparisons (i.e. number of pairwise comparisons within each window divided by the total number of pairwise comparisons) as a function of host genetic distance. Sharing probability was assessed in sliding windows with an interval size of 0.003 and a step size of 0.001 along observed genetic distances.

significantly lower susceptibility than the eight remaining clonal high susceptibility strains (HS, LM, estimate = -3.322 ± 0.081 , $t = -40.609$, $p < 0.001$; Figure 5B). Lower infection could not be attributed to difference in cell-surface phage receptors, as phage 409E50-1 adsorbed to all tested isolates regardless of the production of progeny (Figure S8). We thus concluded that an intracellular defence system found in LS strains controls the efficiency of phage 409E50-1 infection, while other phages from the same species are able to counteract this defence.

Genome comparisons revealed 276 genes that were present in all LS but absent in all HS strains (Table S4). Among these we found two known phage

defence systems, the phosphothioation-sensing bacterial defence system (sspBCDE) targeting viral DNA (Xiong et al., 2020) and the cyclic-oligonucleotide-based anti-phage signalling systems (CBASS_I) leading to host suicide (Millman et al., 2020). However, the double deletion of these systems in 36_P_168 did not change the susceptibility of the host (not shown). The defence mechanism(s) of LS acting on 409E50-1 therefore remain(s) to be identified.

We also sought to understand how the other phages of this species escape the LS defence. A phage can escape from host defences by epigenetic or genetic modifications. Phages 409E50-1 and 521E56-1 were isolated from different strains (respectively,

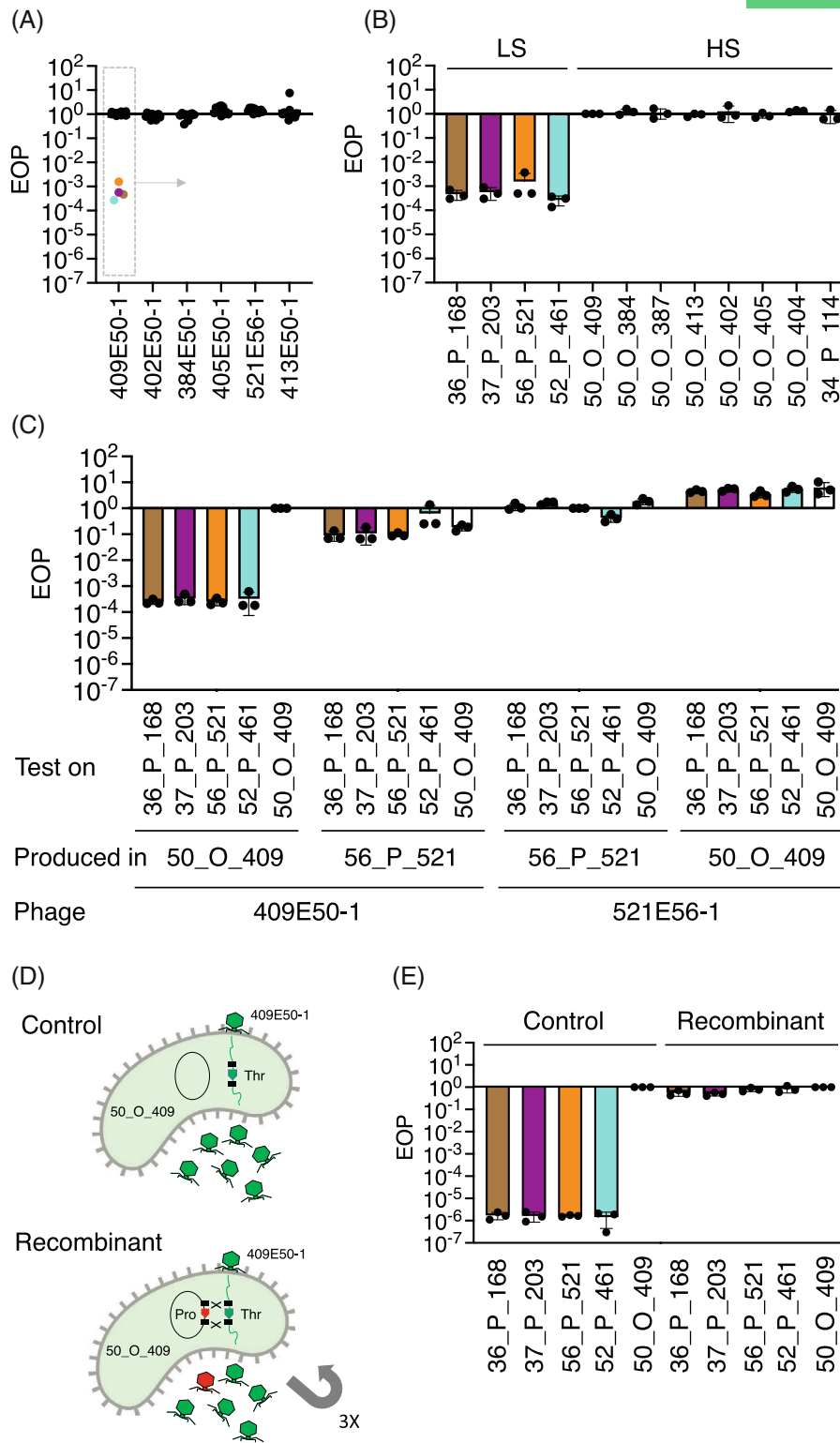


FIGURE 5 Epigenetic and genetic modification are involved in phage adaptation. (A) Efficiency of plating (EOP, the titre of the phage on a given bacteria divided by the titre on the strain used to isolate the phage or ‘original host’) of six phages from VIRIDIC species 26 (Figure S6) on 12 *V. chagasii* strains. Individual dots correspond to the mean from three independent experiments. (B) EOP of the phage 409E50-1 infecting *V. chagasii* strains with low susceptibility (LS) or high susceptibility (HS). Bar charts show the mean \pm s.d. from three independent experiments (individual dots). (C) EOP obtained using *V. chagasii* strains 50_O_409 (HS) or 56_P_521 (LS) to produce the phages 409E50-1 or 521E56-1. Results were standardized by experiment, that is, the production and testing on the original host was normalized to 1 for each experiment. (D) Graphic summary of the strategy used to exchange the nucleotide T to G and codon Thr to Pro in phage 409E50-1. (E) EOP of the recombinant phages or control infecting the four *V. chagasii* strains with low susceptibility (LS). Results were standardized by experiment, that is, the production in original host (50_0_409) was normalized to 1 for each experiment.

50_O_409 and 56_P_521) and diverge by a single SNP in their genome. To explore the hypothesis of epigenetic modification, we produced these phages in the two host strains (Figure 5C). When phage 409E50-1 was propagated on vibrio 56_P_521, its infectivity for LS strains was strongly increased compared to the progeny obtained from the original host (LM, estimate = 2.016 ± 0.296 , $t = 6.821$, $p = 0.002$). The infectivity of phage 521E56-1 was slightly increased when produced on 50_O_409 compared to its original host (Figure 5C, LM estimate = 0.656 ± 0.062 , $t = 10.62$, $p < 0.001$). However, the effect of 409E50-1 was three times greater than that of 521E56-1, indicating that the latter was less affected by the host used to produce progenies. This suggests that vibrio strain 56_P_521 confers an epigenetic advantage to phage 409E50-1 and we hypothesize that phage 521E56-1 does not require host-mediated modification because of genetic divergence.

Phage 409E50-1 differs from 521E56-1 by a single SNP localized in a gene encoding a protein of unknown function (label VP409E501_p0076 in phage 409E50-1; 125 amino acid) (Figure S7). This SNP results in the change of a threonine (409E50-1) to a proline (521E56-1) at amino acid position 8 (Figure S9). We exchanged the allele T > G in phage 409E50-1 by recombination (see Section [Experimental Procedures](#) and Figure 5D) and subsequently observed a significant decrease in the infectivity of the control phages for LS strains (EOP of 10^{-6} instead of 10^{-4} for the ancestral phage, Figure 5B,C). Irrespective of this difference, control phage infections showed significantly lower EOP on LS strains compared to the original host, 50_O_409 (LM, estimate = -5.843 ± 0.123 , $t = -47.571$, $p < 0.001$). The recombinant phages (T > G) were on average 10^6 fold more infectious than control phages on LS strains and did not differ significantly from the original host, 50_O_409 (Figure 5E, LM, estimate = -0.160 ± 0.120 , $t = -1.327$, $p = 0.196$). We therefore show that a single SNP provides protection from the unknown phage defence system present in LS strains. We speculate that this locus could also be the target for epigenetic protection conferred by the host 56_P_521 to phage 409E50-1.

With this mechanistic understanding of the bacteria–phage infection process, we can hypothesize as to how defence elements could spread in the time series samples. The bloom-like proliferation observed on 25 August most likely resulted from the clonal expansion of a HS strain. The expansion of a *V. chagasii* clone in oysters coincided with the disappearance of *V. crassostreae* in the animals. This could be explained by biotic or abiotic factors that are no longer conducive to the replication of *V. crassostreae* in the oyster, leaving this niche accessible to the expansion of another population (population shift). Finally, the clonal expansion presumably drove the overproportional increase of phages assigned to species

26. It is conceivable that this large phage population generated genetic diversity by mutation, including the previously identified SNP that led to adaptation to the host defence system. This adaptation enabled the predominant phages to reproduce in LS strains after the HS bloom and persist for prolonged periods also outside of the oyster environment.

CONCLUSION

In this study, we explored how different genetic structures of hosts can feed back on host–phage interaction networks and genetic diversity of both hosts and phages. The different genetic structures also reflect differences in host ecology and may therefore also influence phage ecology (host range and population dynamics). Between host species, contrasting patterns of genetic diversity for both host and phage resulted in different structures of the respective phage–bacteria interaction networks. Smaller modules in *V. chagasii* were a consequence of a lower number of clonal hosts. More diverse hosts used as prey will lead to the isolation of more diverse phages. A higher specialization of the phages infecting *V. chagasii* was, however, supported by the highest likelihood to share phages when genetic distances were small. Host blooms result in a high number of phages and we showed that this can generate adaptive genetic variability. Selection can work on this increased variability and may favour variants that can also infect hosts outside the bloom, that were less susceptible to the original phage. The free-living lifestyle of *V. chagasii* with blooms inside and outside oyster hosts may thus increase genetic variability of phages but prevent the formation of modules in this host with low population structure.

AUTHOR CONTRIBUTIONS

Karine Cahier: Investigation (lead); methodology (lead); resources (equal). **Damien Piel:** Investigation (equal); methodology (equal); resources (equal); supervision (equal); writing – original draft (equal); writing – review and editing (equal). **Rubén Barcia-Cruz:** Investigation (equal); methodology (equal); writing – original draft (equal); writing – review and editing (equal). **David Goudenège:** Data curation (equal); formal analysis (equal); investigation (equal); methodology (equal); visualization (equal); writing – original draft (equal); writing – review and editing (equal). **K. Mathias Wegner:** Validation (equal); visualization (equal); writing – original draft (equal); writing – review and editing (equal). **Marc Monot:** Methodology (equal); resources (equal). **Jesus L. Romalde:** Funding acquisition (equal); resources (equal). **Frederique Le Roux:** Conceptualization (lead); data curation (equal); formal analysis (equal); funding acquisition (lead); project administration (lead); supervision (lead); validation

(equal); visualization (equal); writing – original draft (lead); writing – review and editing (lead).

ACKNOWLEDGEMENTS

The authors warmly thank Sylvain Gandon, François Blanquart and Martin Polz for fruitful discussions on the manuscript. The authors are grateful to Ian Probert for proofreading the manuscript. The authors thank Sabine Chenivresse, Sophie Le Panse, the staff of the Ifremer Argenton and Bouin stations and of the ABIMS (Roscoff) and LABGeM (Evry) platforms for technical assistance. The authors thank all members of the ‘GV team’ for support with field sampling. The authors thank Zachary Allouche, Biomix Platform, C2RT, Institut Pasteur (Paris, France) supported by France Génomique (ANR-10-INBS-09) and IBISA. This work was supported by funding from the European Research Council (ERC) under the European Union’s Horizon 2020 research and innovation program (grant agreement No 884988, Advanced ERC Dynamic) and the Agence Nationale de la Recherche (ANR-20-CE35-0014 « RESISTE ») to Frédérique Le Roux. Rubén Barcia-Cruz acknowledges the Spanish Ministerio de Ciencia e Innovación for his FPI predoctoral contract (BES-2017-079730).

CONFLICT OF INTEREST STATEMENT

The authors declare no competing interests.

DATA AVAILABILITY STATEMENT

Sequenced genomes have been deposited under the ENA Project with accession numbers PRJEB53320 for *V. chagasii* and PRJEB53960 for phages. All vibrio strains, phage strains and plasmids are available upon request.

ORCID

Frédérique Le Roux  <https://orcid.org/0000-0002-9112-6199>

REFERENCES

- Bolger, A.M., Lohse, M. & Usadel, B. (2014) Trimmomatic: a flexible trimmer for Illumina sequence data. *Bioinformatics*, 30(15), 2114–2120.
- Breitbart, M., Bonnain, C., Malki, K. & Sawaya, N.A. (2018) Phage puppet masters of the marine microbial realm. *Nature Microbiology*, 3(7), 754–766.
- Brum, J.R. & Sullivan, M.B. (2015) Rising to the challenge: accelerated pace of discovery transforms marine virology. *Nature Reviews. Microbiology*, 13(3), 147–159.
- Bruto, M., James, A., Petton, B., Labreuche, Y., Chenivresse, S., Alunno-Bruscia, M. et al. (2017) *Vibrio crassostreae*, a benign oyster colonizer turned into a pathogen after plasmid acquisition. *The ISME Journal*, 11(4), 1043–1052.
- Buchfink, B., Reuter, K. & Drost, H.G. (2021) Sensitive protein alignments at tree-of-life scale using DIAMOND. *Nature Methods*, 18(4), 366–368.
- Chan, P.P. & Lowe, T.M. (2019) tRNAscan-SE: searching for tRNA genes in genomic sequences. *Methods in Molecular Biology*, 1962, 1–14.
- Cordero, O.X. & Polz, M.F. (2014) Explaining microbial genomic diversity in light of evolutionary ecology. *Nature Reviews. Microbiology*, 12(4), 263–273.
- Cordero, O.X., Ventouras, L.A., Delong, E.F. & Polz, M.F. (2012) Public good dynamics drive evolution of iron acquisition strategies in natural bacterioplankton populations. *Proceedings of the National Academy of Sciences of the United States of America*, 109(49), 20059–20064.
- Cordero, O.X., Wildschutte, H., Kirkup, B., Proehl, S., Ngo, L., Hussain, F. et al. (2012) Ecological populations of bacteria act as socially cohesive units of antibiotic production and resistance. *Science*, 337(6099), 1228–1231.
- Corzett, C.H., Elsherbini, J., Chien, D.M., Hehemann, J.H., Henschel, A., Preheim, S.P. et al. (2018) Evolution of a vegetarian vibrio: metabolic specialization of *Vibrio breoganii* to macroalgal substrates. *Journal of Bacteriology*, 200(15), e00020-18.
- de Lorgeril, J., Lucasson, A., Petton, B., Toulza, E., Montagnani, C., Clerissi, C. et al. (2018) Immune-suppression by OsHV-1 viral infection causes fatal bacteraemia in Pacific oysters. *Nature Communications*, 9(1), 4215.
- De Sordi, L., Khanna, V. & Debarbieux, L. (2017) The gut microbiota facilitates drifts in the genetic diversity and infectivity of bacterial viruses. *Cell Host & Microbe*, 22(6), 801–808 e803.
- Deorowicz, S., Debudaj-Grabysz, A. & Gudys, A. (2016) FAMSA: fast and accurate multiple sequence alignment of huge protein families. *Scientific Reports*, 6, 33964.
- Foxx, J., Tighe, S.W., Nicolet, C.M., Zook, J.M., Byrska-Bishop, M., Clarke, W.E. et al. (2021) Performance assessment of DNA sequencing platforms in the ABRF next-generation sequencing study. *Nature Biotechnology*, 39(9), 1129–1140.
- Froelich, B.A. & Noble, R.T. (2014) Factors affecting the uptake and retention of *Vibrio vulnificus* in oysters. *Applied and Environmental Microbiology*, 80(24), 7454–7459.
- Gordillo Altamirano, F.L. & Barr, J.J. (2019) Phage therapy in the Post-antibiotic era. *Clinical Microbiology Reviews*, 32(2), e00066-18.
- Grazziotin, A.L., Koonin, E.V. & Kristensen, D.M. (2017) Prokaryotic virus orthologous groups (pVOGs): a resource for comparative genomics and protein family annotation. *Nucleic Acids Research*, 45(D1), D491–D498.
- Gurevich, A., Saveliev, V., Vyahhi, N. & Tesler, G. (2013) QUAST: quality assessment tool for genome assemblies. *Bioinformatics*, 29(8), 1072–1075.
- Hehemann, J.H., Arevalo, P., Datta, M.S., Yu, X., Corzett, C.H., Henschel, A. et al. (2016) Adaptive radiation by waves of gene transfer leads to fine-scale resource partitioning in marine microbes. *Nature Communications*, 7, 12860.
- Huerta-Cepas, J., Szklarczyk, D., Heller, D., Hernandez-Plaza, A., Forslund, S.K., Cook, H. et al. (2019) eggNOG 5.0: a hierarchical, functionally and phylogenetically annotated orthology resource based on 5090 organisms and 2502 viruses. *Nucleic Acids Research*, 47(D1), D309–D314.
- Hunt, D.E., David, L.A., Gevers, D., Preheim, S.P., Alm, E.J. & Polz, M.F. (2008) Resource partitioning and sympatric differentiation among closely related bacterioplankton. *Science*, 320(5879), 1081–1085.
- Hussain, F.A., Dubert, J., Elsherbini, J., Murphy, M., VanInsberghe, D., Arevalo, P. et al. (2021) Rapid evolutionary turnover of mobile genetic elements drives bacterial resistance to phages. *Science*, 374(6566), 488–492.
- Hyman, P. & Abedon, S.T. (2009) Practical methods for determining phage growth parameters. *Methods in Molecular Biology*, 501, 175–202.
- Jain, C., Rodriguez, R.L., Phillippy, A.M., Konstantinidis, K.T. & Aluru, S. (2018) High throughput ANI analysis of 90K prokaryotic genomes reveals clear species boundaries. *Nature Communications*, 9(1), 5114.

- Jones, P., Binns, D., Chang, H.Y., Fraser, M., Li, W., McAnulla, C. et al. (2014) InterProScan 5: genome-scale protein function classification. *Bioinformatics*, 30(9), 1236–1240.
- Kauffman, K.M., Brown, J.M., Sharma, R.S., VanInsberghe, D., Elsherbini, J., Polz, M. et al. (2018) Viruses of the Nahant collection, characterization of 251 marine Vibrionaceae viruses. *Scientific Data*, 5(1), 180114.
- Kauffman, K.M., Chang, W.K., Brown, J.M., Hussain, F.A., Yang, J., Polz, M.F. et al. (2022) Resolving the structure of phage-bacteria interactions in the context of natural diversity. *Nature Communications*, 13(1), 372.
- Kortright, K.E., Chan, B.K., Koff, J.L. & Turner, P.E. (2019) Phage therapy: a renewed approach to combat antibiotic-resistant bacteria. *Cell Host & Microbe*, 25(2), 219–232.
- Le Roux, F., Binesse, J., Saulnier, D. & Mazel, D. (2007) Construction of a *Vibrio splendidus* mutant lacking the metalloprotease gene *vsm* by use of a novel counterselectable suicide vector. *Applied and Environmental Microbiology*, 73(3), 777–784.
- Le Roux, F., Davis, B.M. & Waldor, M.K. (2011) Conserved small RNAs govern replication and incompatibility of a diverse new plasmid family from marine bacteria. *Nucleic Acids Research*, 39(3), 1004–1013.
- Le Roux, F., Wegner, K.M., Baker-Austin, C., Vezzulli, L., Osorio, C. R., Amaro, C. et al. (2015) The emergence of vibrio pathogens in Europe: ecology, evolution, and pathogenesis (Paris, 11–12th march 2015). *Frontiers in Microbiology*, 6, 830.
- Le Roux, F., Wegner, K.M. & Polz, M.F. (2016) Oysters and Vibrios as a model for disease dynamics in wild animals. *Trends in Microbiology*, 24(7), 568–580.
- Lemire, A., Goudenege, D., Versigny, T., Petton, B., Calteau, A., Labreuche, Y. et al. (2014) Populations, not clones, are the unit of vibrio pathogenesis in naturally infected oysters. *The ISME Journal*, 9(7), 1523–1531.
- Lemire, A., Goudenège, D., Versigny, T., Petton, B., Calteau, A., Labreuche, Y. et al. (2015) Populations, not clones, are the unit of vibrio pathogenesis in naturally infected oysters. *The ISME Journal*, 9(7), 1523–1531.
- McNair, K., Zhou, C., Dinsdale, E.A., Souza, B. & Edwards, R.A. (2019) PHANOTATE: a novel approach to gene identification in phage genomes. *Bioinformatics*, 35(22), 4537–4542.
- Millman, A., Melamed, S., Amitai, G. & Sorek, R. (2020) Diversity and classification of cyclic-oligonucleotide-based anti-phage signaling systems. *Nature Microbiology*, 5(12), 1608–1615.
- Mistry, J., Chuguransky, S., Williams, L., Qureshi, M., Salazar, G.A., Sonnhammer, E.L.L. et al. (2021) Pfam: the protein families database in 2021. *Nucleic Acids Research*, 49(D1), D412–D419.
- Moraru, C., Varsani, A. & Kropinski, A.M. (2020) VIRIDIC-A novel tool to calculate the intergenomic similarities of prokaryote-infecting viruses. *Viruses*, 12(11), 1268.
- Nguyen, L.T., Schmidt, H.A., von Haeseler, A. & Minh, B.Q. (2015) IQ-TREE: a fast and effective stochastic algorithm for estimating maximum-likelihood phylogenies. *Molecular Biology and Evolution*, 32(1), 268–274.
- Nobrega, F.L., Costa, A.R., Kluskens, L.D. & Azeredo, J. (2015) Revisiting phage therapy: new applications for old resources. *Trends in Microbiology*, 23(4), 185–191.
- Perrin, A. & Rocha, E.P.C. (2021) PanACoTA: a modular tool for massive microbial comparative genomics. *NAR: Genomics and Bioinformatics*, 3(1), lqaa106.
- Petton, B., Bruto, M., James, A., Labreuche, Y., Alunno-Bruscia, M. & Le Roux, F. (2015) *Crassostrea gigas* mortality in France: the usual suspect, a herpes virus, may not be the killer in this polymicrobial opportunistic disease. *Frontiers in Microbiology*, 6, 686.
- Piel, D., Bruto, M., James, A., Labreuche, Y., Lambert, C., Janicot, A. et al. (2020) Selection of *Vibrio crassostreae* relies on a plasmid expressing a type 6 secretion system cytotoxic for host immune cells. *Environmental Microbiology*, 22(10), 4198–4211.
- Piel, D., Bruto, M., Labreuche, Y., Blanquart, F., Goudenege, D., Barcia-Cruz, R. et al. (2022) Phage-host coevolution in natural populations. *Nature Microbiology*, 7(7), 1075–1086.
- Preheim, S.P., Timberlake, S. & Polz, M.F. (2011) Merging taxonomy with ecological population prediction in a case study of Vibrionaceae. *Applied and Environmental Microbiology*, 77(20), 7195–7206.
- Rubio, T., Oyanedel, D., Labreuche, Y., Toulza, E., Luo, X., Bruto, M. et al. (2019) Species-specific mechanisms of cytotoxicity toward immune cells determine the successful outcome of *Vibrio* infections. *Proceedings of the National Academy of Sciences of the United States of America*, 116(28), 14238–14247.
- Shapiro, B.J., Friedman, J., Cordero, O.X., Preheim, S.P., Timberlake, S.C., Szabo, G. et al. (2012) Population genomics of early events in the ecological differentiation of bacteria. *Science*, 336(6077), 48–51.
- Smyshlyayev, G., Bateman, A. & Barabas, O. (2021) Sequence analysis of tyrosine recombinases allows annotation of mobile genetic elements in prokaryotic genomes. *Molecular Systems Biology*, 17(5), e9880.
- Stamatakis, A. (2006) RAxML-VI-HPC: maximum likelihood-based phylogenetic analyses with thousands of taxa and mixed models. *Bioinformatics*, 22(21), 2688–2690.
- Steinegger, M. & Soding, J. (2018) Clustering huge protein sequence sets in linear time. *Nature Communications*, 9(1), 2542.
- Szabo, G., Preheim, S.P., Kauffman, K.M., David, L.A., Shapiro, J., Alm, E. J. et al. (2012) Reproducibility of Vibrionaceae population structure in coastal bacterioplankton. *The ISME Journal*, 7(3), 509–519.
- Tesson, F., Herve, A., Mordret, E., Touchon, M., d'Humieres, C., Cury, J. et al. (2022) Systematic and quantitative view of the antiviral arsenal of prokaryotes. *Nature Communications*, 13(1), 2561.
- Vallenet, D., Calteau, A., Dubois, M., Amours, P., Bazin, A., Beuvin, M., et al. (2020) MicroScope: an integrated platform for the annotation and exploration of microbial gene functions through genomic, pangenomic and metabolic comparative analysis. *Nucleic Acids Research*, 48(D1), D579–D589.
- Wang, L., Chen, S., Vergin, K.L., Giovannoni, S.J., Chan, S.W., DeMott, M.S. et al. (2011) DNA phosphorothioation is widespread and quantized in bacterial genomes. *Proceedings of the National Academy of Sciences of the United States of America*, 108(7), 2963–2968.
- Xiong, X., Wu, G., Wei, Y., Liu, L., Zhang, Y., Su, R. et al. (2020) SspABCD-SspE is a phosphorothioation-sensing bacterial defence system with broad anti-phage activities. *Nature Microbiology*, 5(7), 917–928.
- Yawata, Y., Cordero, O.X., Menolascina, F., Hehemann, J.H., Polz, M.F. & Stocker, R. (2014) Competition-dispersal tradeoff ecologically differentiates recently speciated marine bacterioplankton populations. *Proceedings of the National Academy of Sciences of the United States of America*, 111(15), 5622–5627.

SUPPORTING INFORMATION

Additional supporting information can be found online in the Supporting Information section at the end of this article.

How to cite this article: Cahier, K., Piel, D., Barcia-Cruz, R., Goudenège, D., Wegner, K.M., Monot, M. et al. (2023) Environmental vibrio phage–bacteria interaction networks reflect the genetic structure of host populations. *Environmental Microbiology*, 25(8), 1424–1438. Available from: <https://doi.org/10.1111/1462-2920.16366>